ACS central science

Research Article

Cite This: ACS Cent. Sci. 2018, 4, 1394−1402

http://pubs.acs.org/journal/acscii

Delivery of Inorganic Polyphosphate into Cells Using Amphipathic Oligocarbonate Transporters

Gabriella M. Fernandes-Cunha,[†,∥] Colin J. McKinlay,[†,∥] Jessica R. Vargas,[†] Henning J. Jessen,[§] Robert M. Waymouth,[†] and Paul A. Wender*[,†,‡]

[†]Department of Chemistry and [‡]Department of Chemical and Systems Biology, Stanford University, Stanford, California 94305, United States

[§]Institute of Organic Chemistry, Albert-Ludwigs University, Freiburg Albertstr. 21, 79104 Freiburg, Germany

Supporting Information

ABSTRACT: Inorganic polyphosphate (polyP) is an often-overlooked biopolymer of phosphate residues present in living cells. PolyP is associated with many essential biological roles. Despite interest in polyP's function, most studies have been limited to extracellular or isolated protein experiments, as polyanionic polyP does not traverse the nonpolar membrane of cells. To address this problem, we developed a robust, readily employed method for polyP delivery using guanidinium-rich oligocarbonate transporters that electrostatically complex polyPs of multiple lengths, forming discrete nanoparticles that are resistant to phosphatase degradation and that readily enter multiple cell types. Fluorescently labeled polyPs have been monitored over time for subcellular localization and release from the transporter, with control over release rates achieved by modulating the transporter identity and the charge ratio of the electrostatic complexes. This general approach to polyP delivery enables the study of intracellular polyP signaling in a variety of applications.

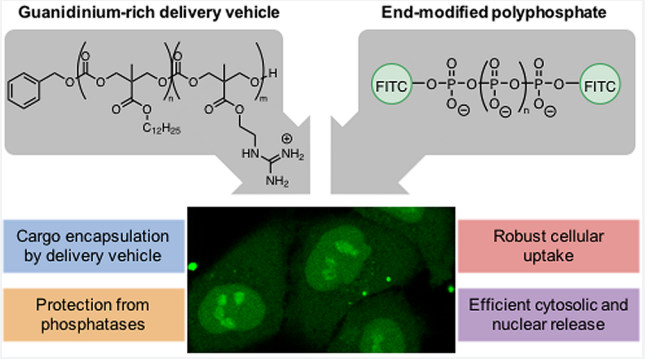

INTRODUCTION

Inorganic polyphosphate (polyP) is an ancient and rarely mentioned biopolymer present in all life-forms, from bacteria and fungi to plants and animals.[1,2] PolyP exists as linear chains of tens to hundreds of orthophosphate residues, all linked by high-energy phosphoanhydride bonds. Despite its evolutionary conservation, polyP is still poorly understood, and new biological activities of this densely anionic molecule are still being uncovered.[3]

In prokaryotic cells, polyP can be found on the cell surface, in the periplasm, and in the plasma membrane,[1,2] while in unicellular eukaryotes, it is typically localized in acidic calcium depots called acidocalcisomes.[4] In mammals, polyP has been found in the brain, heart, liver, kidneys, and lung tissue, as well as in platelets and osteoblast cells.[5−7] PolyP activity has been studied extensively in bacteria and yeast, where its concentrations are much higher than in eukaryotes.[2,8] Several diverse mammalian functions have been observed for polyP, although the details of its signaling remain unclear. PolyP has been shown to interact with mammalian target of rapamycin (mTOR),[9,10] and to influence mitochondrial metabolism.[11] More recently, roles for polyP have been identified in an oxidative stress response,[12] cell metastasis and neovascularization,[13] mineralization of bone cells,[14] apoptosis in plasma cells,[15] as well as in hemostasis and thrombosis.[16] PolyP has also been shown to function as a general chaperone in cells, binding with misfolded proteins to facilitate their refolding.[17] Recently, polyP was discovered to affect cell metabolism by amplifying the production of ATP in the mitochondria.[11] Moreover, polyP transfer to proteins has been established as a new post-translational modification.[18−20] These discoveries have led to an increased interest in understanding polyP signaling, but due to a lack of robust methods to deliver polyP into cells, most of these studies have involved extracellular pathways or biochemical experiments using purified proteins, which greatly limits their scope.

The ability to study the effects of polyP in living cells is hampered by its limited ability to be functionalized, its susceptibility to phosphatase degradation, and most significantly by its inability to cross nonpolar cellular membranes due to its large size and highly anionic charge density. Therefore, new strategies for delivering polyP are required to enable the study of the intracellular functions of this enigmatic molecule. Toward this end, several preliminary studies have evaluated methods by which intracellular delivery of polyP might be achieved, including preparing nanoparticles generated by precipitation with calcium ions,[21,22] forming liposomes,[23] and adsorbing polyP onto gold and silica nanoparticles.[24,25] PolyP nanoparticle formation by nanoprecipitation has been the most

Received: July 16, 2018
Published: September 26, 2018

DOI: 10.1021/acscentsci.8b00470
ACS Cent. Sci. 2018, 4, 1394−1402

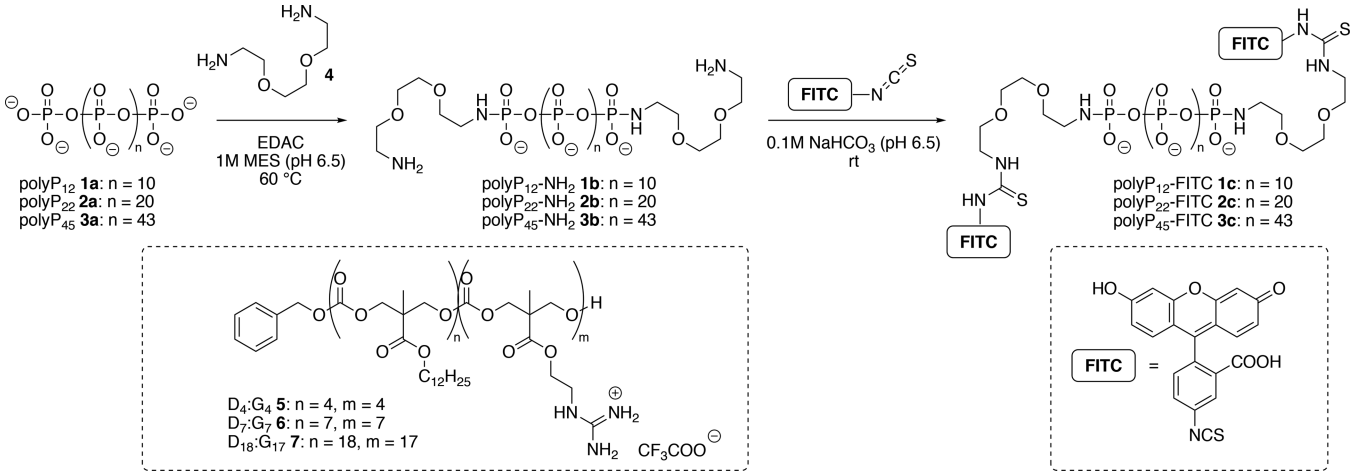

Figure 1. Oligocarbonate transporters and FITC-labeled cargo used for the evaluation of polyP delivery. (A) Synthesis of fluorescently tagged polyP-FITC conjugates by phosphoramidate end-labeling. (B) Previously reported oligocarbonate molecular transporters used for siRNA[30] and $InsP_7$[32] delivery.

common method of delivering polyP intracellularly. Müller and co-workers reported an increased expression of the gene for alkaline phosphatase after incubation of osteoblasts with these nanoparticles.[26] More recently, calcium/polyP nanoparticles were also found to promote osteogenic and chondrogenic differentiation of bone marrow cells.[27] However, many fundamental questions remain, including how polyP is distributed intracellularly after uptake, if there is any difference in polyP uptake among different cell types, how stable polyP particles are to enzymatic degradation, and what the roles of polyP are in cellular function. In addition, these methods to deliver polyP afforded minimal or unreported levels of cellular delivery and are yet to enable widespread study of intracellular polyP signaling and function.

Building on our earlier studies on cell penetrating guanidinium-rich molecular transporters,[28,29] we reported in 2009 that the then new guanidinium-functionalized oligocarbonate molecular transporters were highly effective in complexing, delivering, and releasing linear polyanionic cargos such as siRNA[30,31] and more recently the charge-dense branched polyanion diphospho-myo-inositol pentakisphosphate ($InsP_7$)[32] into cells. The positively charged guanidinium groups on these new vectors served to bind the polyanionic cargo through electrostatic and hydrogen bonding interactions. These novel transporters are easily accessed using a metal-free, organocatalytic ring-opening oligomerization strategy to produce guanidinium-functionalized oligocarbonates in only two steps, irrespective of transporter length or composition,[33,34] and have since been expanded to include materials for the delivery of messenger-RNA[35,36] and plasmid DNA.[37] While differing significantly from oligonucleotides and $InsP_7$ in charge distribution, topology, and conformation, we reasoned that a similar but hitherto unexplored strategy could be used to enable the cellular delivery of polyP. Here we report the intracellular delivery and release of end-modified polyP through complexation with guanidinium-rich molecular transporters. This is the first study that quantitatively and qualitatively demonstrates the delivery of polyP to cells and provides an indication of intracellular distribution of polyP after uptake.

To optically follow polyP uptake and dynamics, polyphosphates of three different average lengths (12, 22, and 45 phosphate units) were reacted with a fluorophore in a two-step sequence (Figure 1A), and the resulting conjugates were systematically evaluated for intracellular delivery using a series of amphipathic (diblock) oligocarbonate transporters (Figure 1B). The generality of polyP delivery was further explored in a panel of cultured cell lines (iPSCs, HeLa, cardiomyocytes, HEK-293, HCT-116). We found that the degree of polyP delivery was independent of polyP length over the lengths studied, but it was significantly impacted by transporter composition and length. Following delivery, polyP localization was visualized using confocal microscopy, which showed that the particles degrade over 18 h to release free polyP into the cytoplasm. Moreover, the rate of polyP release from electrostatic polyplexes can be tuned and controlled by changing parameters such as the charge ratio of transporter to polyP, with release rates ranging from 2 to 24 h. Furthermore, the complexes formed between the transporter and polyP were resistant to alkaline phosphatase activity for multiple hours. This versatile and readily applied method for intracellular polyP delivery serves as an important tool to study and characterize new polyP functions in mammalian cells with potential applications to therapeutic function.

RESULTS AND DISCUSSION

Preparation of Labeled PolyP. Experiments directed at the delivery of polyP require a robust method for quantifying cellular uptake and release. The conjugation of polyP to a fluorescent probe was performed to enable this quantification. Fluorescein isothiocyanate (FITC) conjugates of polyP were prepared using polyPs containing an average of 12, 22, and 45 phosphate units (Figure 1A). Each polyP was first reacted with a diamine linker (**4**), followed by reaction with FITC to provide a fluorescent conjugate. Reaction of polyP with the diamine prior to FITC conjugation prevented the formation of undesired side reactions between the carboxylate and/or phenolic groups of FITC.

To prepare diamine-linked polyP samples **1b**−**3b**, polyP 12, 22, and 45 were coupled to 2,2-(ethylenedioxy)bis-(ethylamine) **4** by 1-ethyl-3-(3-dimethylaminopropyl)-carbodiimide-mediated (EDAC-mediated) phosphoramide coupling using a procedure modified from Hebbard et al.[38] The ^{31}P NMR spectra of the resulting bis-phosphoramide end-

DOI: 10.1021/acscentsci.8b00470
ACS Cent. Sci. 2018, 4, 1394−1402

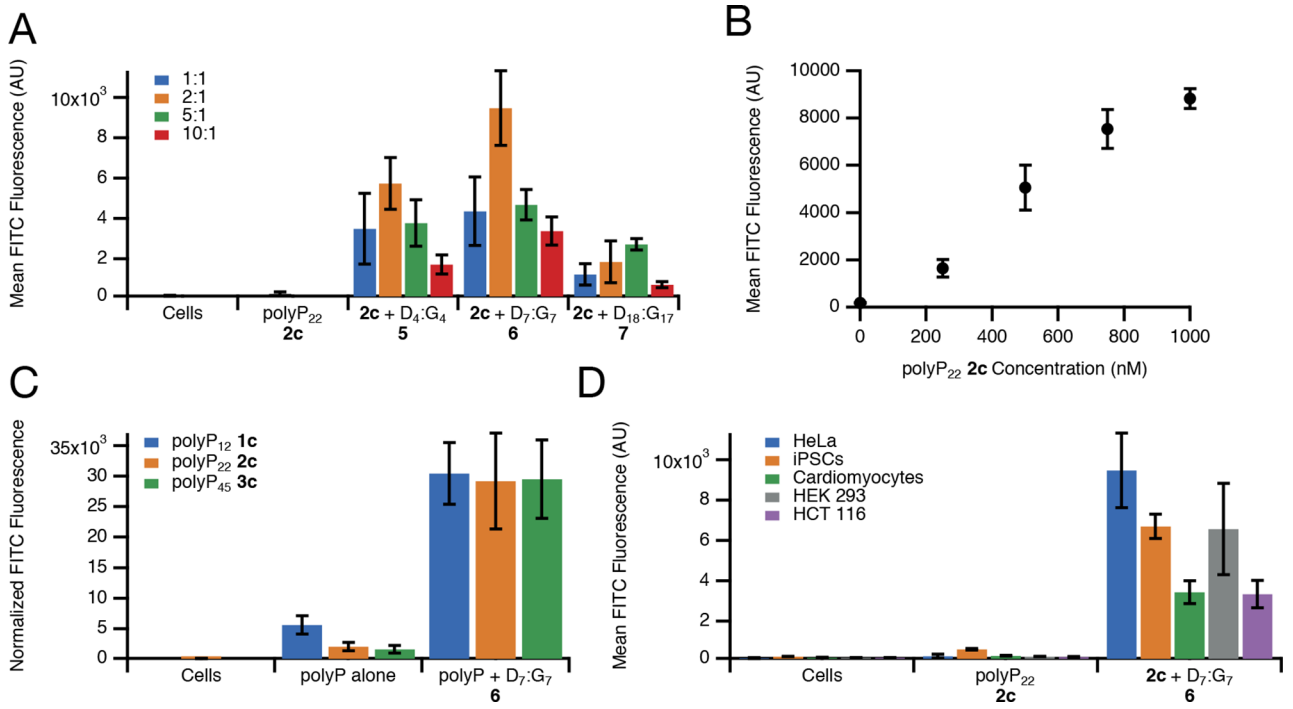

Figure 2. Evaluation of oligocarbonate transporters for polyP-FITC delivery. (A) Delivery of $polyP_{22}$-FITC **2c** alone and complexed with D_4:G_4 **5**, D_7:G_7 **6**, and D_{18}:G_{17} **7** at varying cation:anion charge ratios. (B) Linear dose-dependence of $polyP_{22}$-FITC delivery by D_7:G_7 **6**. (C) Comparison of delivery of varying lengths of polyP (**2a**−**2c**) complexed with D_7:G_7 **6**. Cellular uptake values are normalized to the % FITC labeling determined by NMR and fluorimetry in Figure S2. (D) Delivery of $polyP_{22}$-FITC **2c** complexed with D_7:G_7 6 to multiple cell lines. iPSCs = induced pluripotent stem cells. All flow cytometry data was recorded 4 h after treatment. Data represents the average of three separate experiments ± standard deviation.

capped polyP conjugates showed complete conversion to polyP-diamines **1b**−**3b**, as determined by the appearance of the characteristic P−N resonance at −2.0 ppm. The polyP-diamines were purified by precipitation into ethanol, rather than acetone[39] to avoid imine formation, which was identified as a side reaction with acetone. In order to fully remove excess diamine **4**, which can electrostatically interact with anionic polyP molecules upon protonation, we found that increasing the pH of the reaction to 9.0 prior to precipitation was necessary. Using this strategy, full elimination of diamine was possible, allowing for efficient purification of the resulting conjugates. This modified strategy serves as a foundation for future efforts involving conjugation of polyP to drugs or probes.

To prepare the requisite fluorescent reporter needed to assay polyP delivery by flow cytometry, polyP-diamines **1b**−**3b** were reacted with FITC to obtain polyP-diamine-FITC **1c**−**3c**. The final conjugate was purified by precipitation into ethanol to remove excess FITC, then by preparative size exclusion chromatography. To confirm the absence of unconjugated FITC in the polyP-diamine-FITC samples, agarose gel electrophoresis was run, and no band corresponding to free FITC was observed (Figure S1). Using these methods, polyP conjugates were prepared with modest levels of FITC incorporation suitable for flow cytometry analysis. The efficiency of FITC labeling was determined by NMR end group analysis of FITC resonances relative to diamine, and fluorimetry measurements relative to a calibration curve (Figure S2). Flow cytometry fluorescence values were normalized to the % FITC incorporation of each polyP sample to ensure accurate comparisons of uptake between polyP molecules of different lengths. These methods allowed for the production of mg quantities of fluorescent conjugates for the evaluation of our delivery methods, which could enable future development of polyP-drug or polyP-probe conjugates for imaging and therapy.

Complexation and Delivery of PolyP to Cells. To evaluate amphipathic guanidinium-rich oligocarbonates as transporters for delivering polyP, the ability of these cationic materials to form electrostatic polyplexes with the anionic polyP-FITC cargos **1c**−**3c** was first evaluated. For these experiments, we selected three top-performing transporters from our work on siRNA delivery,[30,31] hypothesizing that they might also be effective for the delivery of this structurally different polyanion (Figure 1B). These oligocarbonate transporters have been shown to complex and deliver polyanions to cells via endocytosis of the resulting electrostatic nanoparticles.[30,31] Polyplex formation was evaluated using an electrophoretic motility assay similar to those used in the oligonucleotide delivery literature.[30,31,40] Free polyP-FITC migrates through an agarose gel toward the positive electrode. The resulting bands can be visualized using UV illumination of the attached FITC fluorophore. When $polyP_{22}$-FITC was mixed with cationic transporter, D_7:G_7 **6**, the charge neutralization of the complex prevented polyP migration, resulting in fluorescence only localized around the loading well and indicating that a stable complex was formed (Figure S3).

Once successful complexation of polyP-FITC conjugates to oligocarbonate transporters was demonstrated, flow cytometry was used to evaluate the uptake of these polyplexes into HeLa cells. Our previous work on siRNA delivery using these transporters showed that optimal gene knockdown occurred using the shortest transporter, D_4:G_4 **5**, at a 4.8:1 charge ratio (cation:anion).[30,31] However, we hypothesized that these

DOI: 10.1021/acscentsci.8b00470
ACS Cent. Sci. 2018, 4, 1394−1402

previous delivery parameters are likely different for polyP, which has much higher charge density, a different charge distribution, and a different structure than siRNA. Therefore, we tested three transporters (D_4:G_4 **5**, D_7:G_7 **6**, and D_{18}:G_{17} **7**) for delivery of $polyP_{22}$-FITC **2c** at charge ratios of 1:1, 2:1, 5:1, and 10:1. Cellular delivery was then quantified by FITC fluorescence using flow cytometry and compared to uncomplexed $polyP_{22}$-FITC **2c** (Figure 2A–D).

As expected for a large polyanion, $polyP_{22}$-FITC **2c** did not appreciably enter cells after 4 h of incubation (Figure 2A). This additionally confirms that any extracellular hydrolysis of $polyP_{22}$-FITC does not result in cellular uptake of free FITC which would be seen as a false-positive in subsequent experiments. In fact, the prior literature supports the fact that FITC alone or small-molecule FITC conjugates are not cell-permeant.[41,42] In stark contrast, all three $polyP_{22}$-FITC **2c**/transporter complexes produced significant levels of FITC fluorescence arising from delivered $polyP_{22}$-FITC **2c**. Intracellular FITC fluorescence was assigned to $polyP_{22}$-FITC (rather than free FITC resulting from hydrolysis of the polyP conjugates) based on previously reported observations that cellular efflux of FITC occurs with a half-life of approximately 30 min, much shorter than the 4 h observation period of these experiments.[43,44] Successful intracellular delivery was further confirmed using 4′,6-diamidino-2-phenylindole (DAPI) staining for intracellular polyP according to a procedure originally reported by Morrissey and adapted to cellular imaging by Aschar-Sobbi et al.[45,46] Cells treated with unconjugated $polyP_{22}$ **2a** complexed with D_7:G_7 **6** showed positive staining for DAPI fluorescence excited at 405 nm which is known to be selective for polyP binding over nucleic acids (Figure S4).

At any given charge ratio, the highest levels of cellular uptake were achieved using transporter D_7:G_7 **6**, followed by D_4:G_4 **5** and D_{18}:G_{17} **7**. This is significant, because the highest levels of siRNA-induced gene knockdown were achieved using the shortest length oligomer, D_4:G_4 **5**,[30] indicating that delivery by guanidinium-rich oligocarbonates is dependent on not only the anionic charge of the cargo but also its charge spacing. Delivery of the highly phosphorylated $InsP_7$ was also most efficient using the longer D_7:G_7 **6**, a finding consistent with cargos possessing higher anionic charge densities requiring complexing agents with more cationic charges.[32]

In addition to the dependence on transporter length, we evaluated the effect of charge ratio between the guanidinium cations on the transporter and the phosphate anions on cellular delivery of $polyP_{22}$-FITC **2c**. The delivery of $polyP_{22}$-FITC **2c** by three transporters exhibited a parabolic dependence on cation:anion charge ratio. Uptake was highest at a 2:1 ratio for D_4:G_4 **5** and the top-performing D_7:G_7 **6**, while D_{18}:G_{17} **7** showed slightly better uptake at 5:1. In another departure from siRNA observations, this 2:1 ratio was lower than the cation:anion ratios used for siRNA delivery, where it was found that a 4.8:1 charge ratio induced maximal gene knockdown. This difference is potentially due to the differences in charge distribution between the densely polyanionic polyP as an inorganic salt, compared to a more diffuse, organo-polyanion such as siRNA. The parabolic uptake profile as a function of charge ratio could be a consequence of lower amounts of cation not being sufficient to form electrostatic complexes with polyP (due to fewer positive charges), while higher ratios afford particles that are too cationic to be efficiently taken into cells. The influence of different cargo charge densities on particle formation and cellular uptake will be explored in future studies.

As a result of these experiments, D_7:G_7 **6** at a 2:1 charge ratio was identified as the optimal polyP delivery vehicle, and these conditions were used in subsequent uptake studies. $PolyP_{22}$-FITC delivery by D_7:G_7 **6** showed a linear dependence on treatment concentration from 250 to 1000 nM by flow cytometry (Figure 2B). This will allow for control over treatment concentration in future studies of polyP pathways and/or therapeutic applications.

Following preliminary delivery experiments conducted with a single polyP length, $polyP_{22}$-FITC **2c**, we sought to further evaluate whether D_7:G_7 **6** was an efficient delivery vehicle for other polyP sizes. For these studies, the cellular fluorescence values by flow cytometry were normalized to the percent FITC end-labeling determined previously (Figure S2) to ensure an accurate comparison. When complexes were formed with $polyP_{12}$-FITC **1c** and $polyP_{45}$-FITC **3c**, nearly equivalent levels of intracellular FITC fluorescence were observed (Figure 2C). This indicates that our delivery strategy is not significantly dependent on the number of phosphate units within a polyP molecule, but rather, delivery is general for multiple lengths. Based on this preliminary data, we can reason that the delivery would be maintained for longer polyP chains as well.

To confirm that the delivery of polyP is general across multiple cell lines, we tested the uptake of these complexes in induced pluripotent stem cells (iPSCs),[47] cardiomyocytes,[48] HEK-293, and HCT-116, in addition to the optimization experiments done in HeLa cells (Figure 2D). These cell types were selected based on potential applications of these transporters for studying polyP pathways and therapeutic effects, including polyP-induced proliferation of iPSC-derived odontoblast-like cells,[49] and polyP-related protection of cardiomyocytes after ischemia and reperfusion or myocardial infarction.[50] In all of these cell lines, D_7:G_7 **6** effected high levels of polyP uptake, while uncomplexed polyP showed no significant uptake, providing a foundation for using this delivery strategy as a tool for studying intracellular polyP function in multiple cell types.

Release of PolyP from Oligocarbonate Complexes. A gel shift assay was also used to further explore the release of polyP from amphipathic oligocarbonate complexes. The release of polyP was assessed by gel retardation assay with a reappearance of a free polyP band indicating polyplex degradation and polyP release. The release was evaluated in a window from 2 to 24 h at 37 °C. These experiments were conducted with $polyP_{22}$ due to its intermediate length. In the first experiment, the highest-performing co-oligomer, D_7:G_7 **6**, was incubated with FITC-$polyP_{22}$ at cation:anion charge ratios of 1:1, 2:1, 5:1, and 10:1. At charge ratios of 10:1 and 5:1, the complexes were stable for 8 h, and release was observed at 24 h due to complex degradation (Table 1, Figure S5A). However,

Table 1. Gel Shift Release Times of PolyP Complexed with Guanidinium-Rich Transporters at Several Charge Ratios

	transporter		
± charge ratio	D_4:G_4 **5**	D_7:G_7 **6**	D_{18}:G_{17} **7**
1:1		2–4 h	
2:1	6–8 h	6–8 h	1–2 h
5:1		8–24 h	
10:1		8–24 h	

DOI: 10.1021/acscentsci.8b00470
ACS Cent. Sci. 2018, 4, 1394–1402

complexes formed at charge ratios of 2:1 and 1:1 were less stable, with release occurring between 4 and 8 h. Release of polyanions from electrostatic complexes has been previously shown to correlate with the hydrolytic stability of the cationic transporter used.[30,51] This behavior additionally suggests that the amount of oligomer present in complexes plays an important role in the release of polyP. When polyplexes are formulated at a higher charge ratio, the increased amount of oligomer present allows for electrostatic interactions to persist even after partial hydrolysis has occurred, resulting in slower release rates. We anticipate that charge ratio is another parameter that can be independently explored to tune release rate in applications where longer or shorter release times are required.

Next, we aimed to determine the effect of co-oligomer length on release rate of $polyP_{22}$ from polyplexes. $PolyP_{22}$ was incubated with D_4:G_4 **5**, D_7:G_7 **6**, and D_{18}:G_{17} **7** at a 2:1 charge ratio and its release rate characterized by gel electrophoresis. Interestingly, while D_4:G_4 **5** and D_7:G_7 **6** released $polyP_{22}$ between 6 and 8 h, D_{18}:G_{17} **7** released $polyP_{22}$ after only 1 h (Table 1, Figure S5B). It is possible that this is a result of decreased stability in the complexes formed between D_{18}:G_{17} **7** and polyP due to factors such as packing and/or a destabilizing effect of the much higher lipid content. In conjunction with delivery experiments which showed much lower uptake occurring using D_{18}:G_{17} **7** relative to D_4:G_4 **5** and D_7:G_7 **6**, these results suggest that particles with the former might not be stable enough to produce significant cellular uptake or that polyplex degradation and polyP release occur too quickly for substantial amounts of polyP to be delivered.

The tunable properties of our delivery system allow for its potential use in a variety of delivery scenarios. For instance, conditions which release polyP quickly could be advantageous for applications involving blood coagulation.[52] Conversely, a recent report evaluated the antiangiogenic activity of polyP, where prolonged polyP release could be used to treat eye diseases such as degenerative macular edema.[13]

Intracellular Release and Distribution of PolyP. In addition to exploring polyP release using gel assays, we used FITC-polyP to evaluate intracellular polyP release after delivery by oligocarbonate complexes. In this study, HeLa cells were treated with either $polyP_{22}$-FITC **2c** alone or polyplexes formed with D_7:G_7 **6** and imaged by confocal microscopy immediately, or after 18 h of incubation (Figure 3). Cells treated with $polyP_{22}$-FITC **2c** alone exhibited only minimal levels of FITC fluorescence at both 4 and 18 h, confirming flow cytometry results. In contrast, HeLa cells treated with polyplexes showed high levels of intracellular FITC fluorescence at both time points. This data confirms that flow cytometry results are accurate quantifications of intracellular $polyP_{22}$-FITC **2c** and not the result of particles adhered to the cell surface. Interestingly, after 4 h, the FITC fluorescence is highly localized in bright puncta, with the bulk of the cell body remaining relatively unstained. This is consistent with endocytotic uptake of polyplexes which have not yet degraded on such a short time scale, and is supported by prior mechanistic studies with these amphipathic oligocarbonates for polyanion delivery.[30,32] Significantly, after 18 h, nearly all of the bright puncta had disappeared, and fluorescence was much more diffuse in appearance, consistent with the previously determined release rate of $polyP_{22}$ complexed with D_7:G_7 **6** over 12−20 h. The diffuse nature of this fluorescence confirms the ability of our transporters to

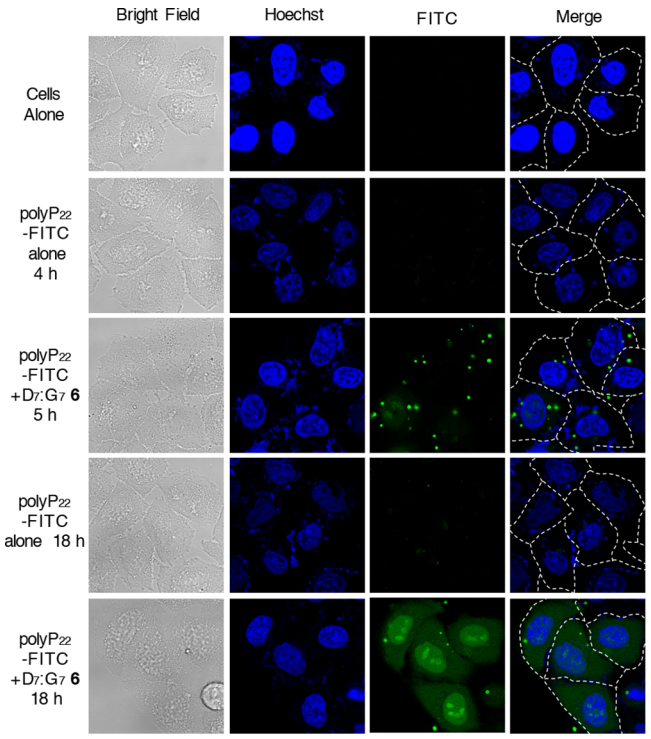

Figure 3. Confocal microscopy images of cells treated with $polyP_{22}$-FITC alone and complexed with D_7:G_7 **6**. Imaging was performed 4 and 18 h following treatment. Cell nuclei were stained with Hoechst 33342. Dotted lines in merged images are cell body outlines taken from bright field images.

not only deliver polyP but also release it intracellularly. Furthermore, FITC-polyP fluorescence seems to show higher levels of fluorescence in the nucleus and nucleolus, which supports observations by Kornberg demonstrating accumulation of polyP in those subcellular structures.[5] Nuclear localization is suggestive of one of polyP's hypothesized functions of affecting gene expression by disrupting nucleohistone complexes.[53] This distribution is particularly interesting, in this case, because it is in stark contrast with other FITC-labeled anions such as siRNA which tend to show only cytosolic fluorescence and exclude the nucleus.[30,54,55]

Protection of PolyP from Phosphatase Degradation. An effective drug delivery technology should protect its cargo from the extracellular environment and/or during circulation prior to intracellular delivery. Polyphosphate has previously been shown to undergo cleavage by exopolyphosphatases, as well as by promiscuous extracellular phosphatases.[56,57] Therefore, to test whether our transporter polyplexes would be useful in vitro and in vivo, we investigated their ability to protect the polyP cargo from enzymatic degradation. Protection from phosphatases was determined using an adaptation of a method reported by Lonrez,[56] where degraded polyP was quantified using a malachite green assay.[58] Briefly, complexes were formed between $polyP_{22}$ **2a** and D_7:G_7 **6** and then incubated with varying concentrations of alkaline phosphatase; then, free PO_4^{3-} was measured colorimetrically. Unmodified polyP was used in this study because end-labeled polyP has been shown to be resistant to phosphatase degradation.[39] For this assay, the effect of three different variables on phosphatase degradation was studied: (1) the amount of alkaline phosphatase, (2) the charge ratio of polyplexes, and (3) the exposure time to enzyme. The alkaline phosphatase concentration was evaluated

DOI: 10.1021/acscentsci.8b00470
ACS Cent. Sci. 2018, 4, 1394−1402

over an interval of 4−23 U for 20 min (U, enzyme unit) (Figure S6). As expected, the degree of degradation of polyP alone linearly increased with the enzyme concentration until approximately 13 U, after which no additional degradation occurred. However, when complexed with D_7:G_7 **6**, the polyplexes provided significant protection compared to naked (uncomplexed) polyP, and overall levels of degradation were low. For the following studies, we chose to use an enzyme concentration of 2 U and a 20 min exposure time similar to other reports in the literature.[39] To understand how the charge ratio of oligocarbonate transporter affects the degree of polyP degradation, several charge ratios were evaluated: 0.5:1, 1:1, 2:1, 5:1, and 10:1 (cation:anion, Figure 4A). We observed that

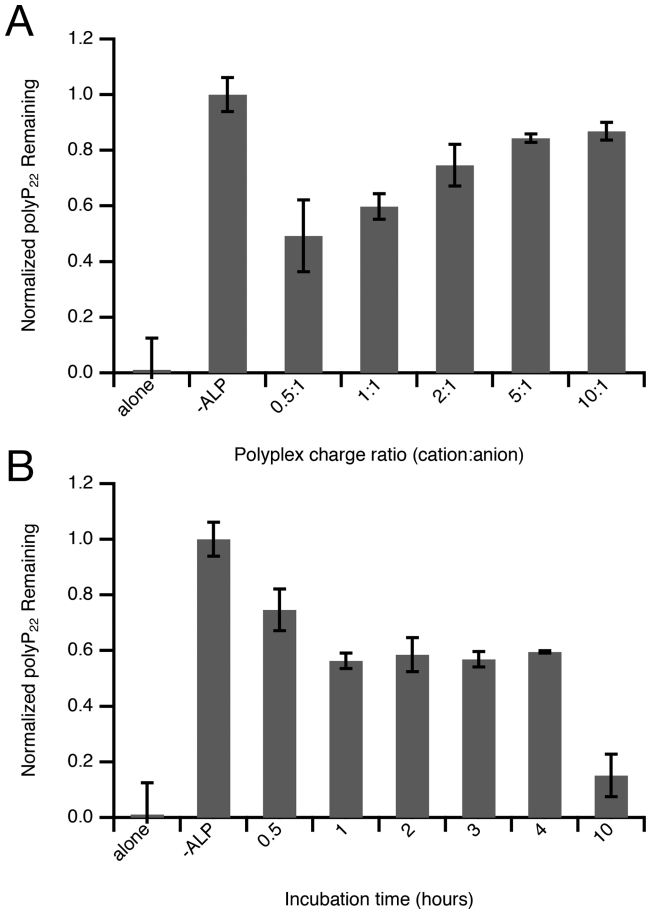

Figure 4. Protection of $polyP_{22}$ cargo from alkaline phosphatase when complexed with D_7:G_7 **6**. (A) Protection of polyP22 complexes as a function of formulation charge ratio (expressed as cation:anion). (B) Protection of polyP22 complexes as a function of time. Polyplexes were incubated for the indicated amount of time at 37 °C prior to exposure to the enzyme.

increasing the charge ratio improved the protection against alkaline phosphatase degradation. This is consistent with our observations that particles formed at lower charge ratios appear to be less electrostatically stable, and thus provide less protection from exogenous agents such as phosphatases.

In our uptake studies, we treated cells with polyP complexes for 4 h to ensure polyP delivery. In this regard, we aimed to see whether the increase in the exposure time to phosphatase from 20 min to 4 h would increase the degradation of polyP complexed with the transporter. Interestingly, increasing the exposure time from 20 min to 1 h degrades a small amount of additional polyphosphate, but from 1 to 4 h, the residual complexed polyP remained stable (Figure 4B). A possible explanation for this is that the polyP degraded in the first hour which is due to loosely bound molecules on the polyplex surface, while the majority of polyP is complexed more tightly in the interior of particles. When polyplexes were incubated for 10 h, significant polyP degradation was observed, which corroborates our previously determined release data for complexes formed with D_7:G_7 **6** consistent with release times on the order of 12−20 h.

Characterization of Polyplexes. Dynamic light scattering (DLS) was used to determine the particle size and ζ potential of the polyplexes formed with D_7:G_7 **6** and polyP. For these measurements, complexes were formed at the optimal charge ratio used for in vitro polyP delivery experiments (2:1 cation:anion). The polyplex size was slightly under 200 nm for all polyphosphate lengths evaluated ($polyP_{12}$, $polyP_{22}$, $polyP_{45}$), indicating that particle size is not significantly affected by cargo size or number of anionic charges (Figure 4A). Previous work has shown that the endocytosis of other oligocarbonate polyplexes, such as those used for oligonucleotides, is most efficient when particle sizes are under 200 nm, so it is reasonable that the same behavior would apply for particles for polyP delivery.[59−61] The similarity in particle sizes is consistent with our uptake results which showed that all polyP molecules were taken up at similar levels. To determine if the functionalization of polyP would impair the particle size, we compared complexes formed with FITC-modified polyP and unmodified polyP. No significant difference in the particle size between unfunctionalized polyP and FITC-polyP conjugates was observed (Figure 4B). Particle sizes were monitored over the course of an hour and showed no evidence of particle aggregation on that time scale, indicating that particles are stable in aqueous buffer solutions.

The ζ potential of all polyplexes was measured to be approximately +20 mV for all polyplexes (Figure 5C,D). This cationic surface charge is reflective of the excess of positive charges used in formulation. Since all complexes were formed at the same charge ratio no difference in the ζ potential would be expected. This slight excess in positive charge helps prevent aggregation while improving endocytosis by increasing interaction with anionic groups (phosphates, sulfates, and carboxylates) on the cellular membrane.

MTT Cell Viability Assay. We have previously shown that the oligocarbonate transporters used here for polyP delivery are not significantly toxic to cells alone or when complexed with siRNA.[30] However, we additionally verified that the polyplexes with polyP do not significantly impact cellular viability. To test this, HeLa cells were incubated with $polyP_{12}$, $polyP_{22}$, and $polyP_{45}$ complexed with D_7:G_7 **6**, and their resulting viability was assessed with an MTT assay. After 48 h, none of the polyP lengths affected cell viability up to high concentrations when directly exposed to the cells (Figure S7). This was expected as polyP is naturally present in cells and does not cross the cell membrane. Cells incubated with polyP/D_7:G_7 **6** polyplexes induced no significant decrease in viability when incubated with up to 1000 nM total polyP concentration. At this level only the $polyP_{45}$ formulation showed some toxicity attributed to the much higher oligomer amounts necessary to achieve a 2:1 charge ratio with longer cargos. This validates our methods as being able to deliver polyP over a wide range of concentrations for a variety of potential applications.

DOI: 10.1021/acscentsci.8b00470
ACS Cent. Sci. 2018, 4, 1394−1402

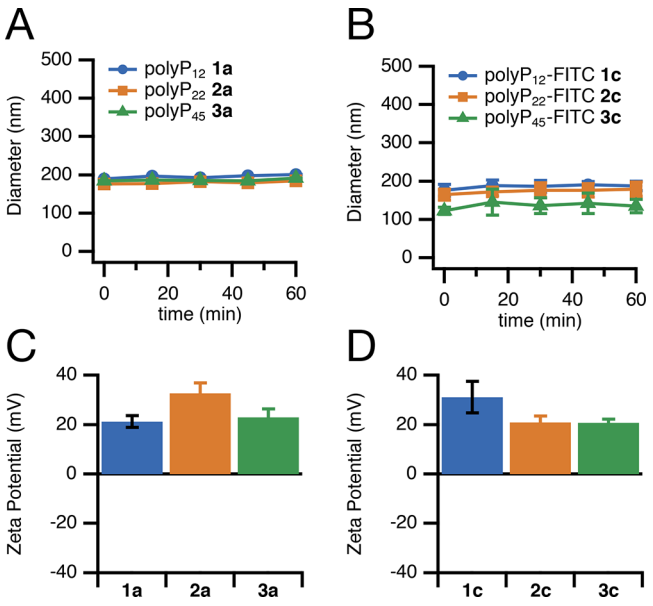

Figure 5. Characterization of polyP polyplexes formed with oligocarbonate transporter D_7:G_7 **6**. (A) DLS-determined sizes of complexes formed with unmodified polyPs **1a**, **2a**, and **3a**. (B) Sizes of complexes formed with polyP-FITC conjugates **1c**, **2c**, and **3c**. (C) ζ potential of unmodified polyP complexes. (D) ζ potential of polyP-FITC complexes. All measurements were taken using transporter **6** complexed at a 2:1 charge ratio (cation:anion) and are reported as mean ± standard deviation (n = 3).

CONCLUSIONS

Signaling and regulation by polyphosphate biopolymers has been implicated in a wide range of biological functions across kingdoms; however, many fundamental questions remain about the nature of its regulation and modes of action. One major challenge associated with studying polyP has been the dearth of methods for its intracellular delivery and detection. Here we present a general strategy for intracellular delivery of polyP by noncovalently complexing this anionic biopolymer with guanidinium-rich oligocarbonate transporters. This represents a fundamentally new structural cargo for these transporters which have been shown previously to work for siRNA and inositol polyphosphate delivery. We have shown that the resulting nanoparticles are biocompatible and protective against phosphatase activity, and they can be delivered into multiple cell lines, including cells known to participate in important polyP functions. These tunable polyplexes can be designed and tuned to achieve a desired rate of polyP release as well as degree of cellular uptake by simply changing the composition of the polyplexes in a modular fashion. While this study focused on three relatively short polyP lengths (12, 22, and 45), our prior work has shown that similar transporter molecules are effective for cargos across broad range of sizes, from siRNA (approximately 13 kDa) to plasmid DNA (>1 MDa) so we are confident that larger polyP sizes could be delivered with minimal procedural changes. The evaluation of the polyplexes following cellular delivery provided information about polyP release and subcellular distribution, and these results will be further explored in future studies. We also have shown that, by using a diamine linker, polyP can be conjugated to different probes or drugs, highlighting its potential applications for imaging and therapeutic strategies. We expect that our strategy will have significant impact in enabling the discovery and evaluation of new polyP functions in multiple settings and advancing our knowledge of this under-explored but ubiquitous fourth class of natural biopolymers.

ASSOCIATED CONTENT

Supporting Information

The Supporting Information is available free of charge on the ACS Publications website at DOI: 10.1021/acscentsci.8b00470.

Additional experimental procedures, characterization information, and figures including gel shift assay, FITC fluorescence curve, DAPI staining, MTT assay, ^{1}H NMR, ^{13}C NMR, and ^{31}P NMR (PDF)

AUTHOR INFORMATION

Corresponding Author

*E-mail: wenderp@stanford.edu. Phone: (650) 723-0208. Fax: (650) 725-0259.

ORCID

Gabriella M. Fernandes-Cunha: 0000-0002-9934-5310
Henning J. Jessen: 0000-0002-1025-9484
Robert M. Waymouth: 0000-0001-9862-9509
Paul A. Wender: 0000-0001-6319-2829

Author Contributions

‖G.M.F.-C. and C.J.M. contributed equally.

Notes

The authors declare no competing financial interest.

ACKNOWLEDGMENTS

This work was supported by Department of Energy Grant DE-SC0018168 and National Science Foundation Grant NSF CHE-1607092 (to R.M.W.), HFSP RGP0025 (to P.A.W. and H.J.J.), and NIH-CA031845 (to P.A.W.). Support through the Stanford Center for Molecular Analysis and Design (CMAD, C.J.M.), the Child Health Research Institute, and SPARK program at Stanford University is further acknowledged. Flow cytometry data was collected on an instrument in the Stanford Shared FACS Facility obtained using NIH S10 Shared Instrument Grant S10RR027431-01. We gratefully acknowledge Prof. Chris Contag and Prof. Sanjiv Sam Gambhir for materials, tissue culture equipment, and use of IVIS system; Prof. Richard Zare for the use of the Malvern Zetasizer DLS; Prof. Chaitan Khosla for use of HeLa cells; and Prof. Joseph Wu for the iPSCs. The authors further acknowledge Dr. Rashna Bhandari (Centre for DNA Fingerprinting and Diagnostics, Bangalore) for advice and insightful discussions.

REFERENCES

(1) Kornberg, A.; Rao, N. N.; Ault-Riché, D. Inorganic Polyphosphate: A Molecule of Many Functions. *Annu. Rev. Biochem.* **1999**, *68*, 89−125.

(2) Brown, M. R. W.; Kornberg, A. Inorganic Polyphosphate in the Origin and Survival of Species. *Proc. Natl. Acad. Sci. U. S. A.* **2004**, *101* (46), 16085−16087.

(3) Morrissey, J. H.; Choi, S. H.; Smith, S. A. Polyphosphate: An Ancient Molecule That Links Platelets, Coagulation, and Inflammation. *Blood* **2012**, *119* (25), 5972−5979.

(4) Lander, N.; Cordeiro, C.; Huang, G.; Docampo, R. Polyphosphate and Acidocalcisomes. *Biochem. Soc. Trans.* **2016**, *44* (1), 1−6.

DOI: 10.1021/acscentsci.8b00470
ACS Cent. Sci. 2018, 4, 1394−1402

(5) Kumble, K. D.; Kornberg, A. Inorganic Polyphosphate in Mammalian Cells and Tissues. *J. Biol. Chem.* **1995**, *270* (11), 5818−5822.
(6) Ruiz, F. A.; Lea, C. R.; Oldfield, E.; Docampo, R. Human Platelet Dense Granules Contain Polyphosphate and Are Similar to Acidocalcisomes of Bacteria and Unicellular Eukaryotes. *J. Biol. Chem.* **2004**, *279* (43), 44250−44257.
(7) Schröder, H. C.; Kurz, L.; Müller, W. E. G.; Lorenz, B. Polyphosphate in Bone. *Biochem. Mosc.* **2000**, *65* (3), 296−303.
(8) Seufferheld, M. J.; Alvarez, H. M.; Farias, M. E. Role of Polyphosphates in Microbial Adaptation to Extreme Environments. *Appl. Environ. Microbiol.* **2008**, *74* (19), 5867−5874.
(9) Wang, L.; Fraley, C. D.; Faridi, J.; Kornberg, A.; Roth, R. A. Inorganic Polyphosphate Stimulates Mammalian TOR, a Kinase Involved in the Proliferation of Mammary Cancer Cells. *Proc. Natl. Acad. Sci. U. S. A.* **2003**, *100* (20), 11249−11254.
(10) Hassanian, S. M.; Dinarvand, P.; Smith, S. A.; Rezaie, A. R. Inorganic Polyphosphate Elicits Pro-Inflammatory Responses through Activation of the Mammalian Target of Rapamycin Complexes 1 and 2 in Vascular Endothelial Cells. *J. Thromb. Haemostasis* **2015**, *13* (5), 860−871.
(11) Abramov, A. Y.; Fraley, C.; Diao, C. T.; Winkfein, R.; Colicos, M. A.; Duchen, M. R.; French, R. J.; Pavlov, E. Targeted Polyphosphatase Expression Alters Mitochondrial Metabolism and Inhibits Calcium-Dependent Cell Death. *Proc. Natl. Acad. Sci. U. S. A.* **2007**, *104* (46), 18091−18096.
(12) Gray, M. J.; Jakob, U. Oxidative Stress Protection by Polyphosphate — New Roles for an Old Player. *Curr. Opin. Microbiol.* **2015**, *24*, 1−6.
(13) Han, K. Y.; Hong, B. S.; Yoon, Y. J.; Yoon, C. M.; Kim, Y.-K.; Kwon, Y.-G.; Gho, Y. S. Polyphosphate Blocks Tumour Metastasis via Anti-Angiogenic Activity. *Biochem. J.* **2007**, *406* (1), 49−55.
(14) Kawazoe, Y.; Shiba, T.; Nakamura, R.; Mizuno, A.; Tsutsumi, K.; Uematsu, T.; Yamaoka, M.; Shindoh, M.; Kohgo, T. Induction of Calcification in MC3T3-E1 Cells by Inorganic Polyphosphate. *J. Dent. Res.* **2004**, *83* (8), 613−618.
(15) Hernandez-Ruiz, L.; González-García, I.; Castro, C.; Brieva, J. A.; Ruiz, F. A. Inorganic Polyphosphate and Specific Induction of Apoptosis in Human Plasma Cells. *Haematologica* **2006**, *91* (9), 1180−1186.
(16) Smith, S. A.; Morrissey, J. H. Polyphosphate: A New Player in the Field of Hemostasis. *Curr. Opin. Hematol.* **2014**, *21* (5), 388−394.
(17) Gray, M. J.; Wholey, W.-Y.; Wagner, N. O.; Cremers, C. M.; Mueller-Schickert, A.; Hock, N. T.; Krieger, A. G.; Smith, E. M.; Bender, R. A.; Bardwell, J. C. A.; et al. Polyphosphate Is a Primordial Chaperone. *Mol. Cell* **2014**, *53* (5), 689−699.
(18) Azevedo, C.; Livermore, T.; Saiardi, A. Protein Polyphosphorylation of Lysine Residues by Inorganic Polyphosphate. *Mol. Cell* **2015**, *58* (1), 71−82.
(19) Bentley-DeSousa, A.; Holinier, C.; Moteshareie, H.; Tseng, Y.-C.; Kajjo, S.; Nwosu, C.; Amodeo, G. F.; Bondy-Chorney, E.; Sai, Y.; Rudner, A.; et al. A Screen for Candidate Targets of Lysine Polyphosphorylation Uncovers a Conserved Network Implicated in Ribosome Biogenesis. *Cell Rep.* **2018**, *22* (13), 3427−3439.
(20) Azevedo, C.; Singh, J.; Steck, N.; Hofer, A.; Ruiz, F. A.; Singh, T.; Jessen, H. J.; Saiardi, A. Screening a Protein Array with Synthetic Biotinylated Inorganic Polyphosphate To Define the Human PolyP-Ome. *ACS Chem. Biol.* **2018**, *13* (8), 1958−1963.
(21) Muller, W. E. G.; Tolba, E.; Feng, Q.; Schroder, H. C.; Markl, J. S.; Kokkinopoulou, M.; Wang, X. Amorphous Ca2+ Polyphosphate Nanoparticles Regulate the ATP Level in Bone-like SaOS-2 Cells. *J. Cell Sci.* **2015**, *128* (11), 2202−2207.
(22) Donovan, A. J.; Kalkowski, J.; Smith, S. A.; Morrissey, J. H.; Liu, Y. Size-Controlled Synthesis of Granular Polyphosphate Nanoparticles at Physiologic Salt Concentrations for Blood Clotting. *Biomacromolecules* **2014**, *15* (11), 3976−3984.
(23) Donovan, A. J.; Kalkowski, J.; Szymusiak, M.; Wang, C.; Smith, S. A.; Klie, R. F.; Morrissey, J. H.; Liu, Y. Artificial Dense Granules: A Procoagulant Liposomal Formulation Modeled after Platelet Polyphosphate Storage Pools. *Biomacromolecules* **2016**, *17* (8), 2572−2581.
(24) Szymusiak, M.; Donovan, A. J.; Smith, S. A.; Ransom, R.; Shen, H.; Kalkowski, J.; Morrissey, J. H.; Liu, Y. Colloidal Confinement of Polyphosphate on Gold Nanoparticles Robustly Activates the Contact Pathway of Blood Coagulation. *Bioconjugate Chem.* **2016**, *27* (1), 102−109.
(25) Kudela, D.; Smith, S. A.; May-Masnou, A.; Braun, G. B.; Pallaoro, A.; Nguyen, C. K.; Chuong, T. T.; Nownes, S.; Allen, R.; Parker, N. R.; et al. Clotting Activity of Polyphosphate-Functionalized Silica Nanoparticles. *Angew. Chem., Int. Ed.* **2015**, *54* (13), 4018−4022.
(26) Müller, W. E. G.; Tolba, E.; Schröder, H. C.; Wang, S.; Glaßer, G.; Muñoz-Espí, R.; Link, T.; Wang, X. A New Polyphosphate Calcium Material with Morphogenetic Activity. *Mater. Lett.* **2015**, *148*, 163−166.
(27) Müller, W.; Neufurth, M.; Wang, S.; Ackermann, M.; Muñoz-Espí, R.; Feng, Q.; Lu, Q.; Schröder, H.; Wang, X. Amorphous, Smart, and Bioinspired Polyphosphate Nano/Microparticles: A Biomaterial for Regeneration and Repair of Osteo-Articular Impairments In-Situ. *Int. J. Mol. Sci.* **2018**, *19* (2), 427.
(28) Wender, P. A.; Mitchell, D. J.; Pattabiraman, K.; Pelkey, E. T.; Steinman, L.; Rothbard, J. B. The Design, Synthesis, and Evaluation of Molecules That Enable or Enhance Cellular Uptake: Peptoid Molecular Transporters. *Proc. Natl. Acad. Sci. U. S. A.* **2000**, *97* (24), 13003−13008.
(29) Stanzl, E. G.; Trantow, B. M.; Vargas, J. R.; Wender, P. A. Fifteen Years of Cell-Penetrating, Guanidinium-Rich Molecular Transporters: Basic Science, Research Tools, and Clinical Applications. *Acc. Chem. Res.* **2013**, *46* (12), 2944−2954.
(30) Geihe, E. I.; Cooley, C. B.; Simon, J. R.; Kiesewetter, M. K.; Edward, J. A.; Hickerson, R. P.; Kaspar, R. L.; Hedrick, J. L.; Waymouth, R. M.; Wender, P. A. Designed Guanidinium-Rich Amphipathic Oligocarbonate Molecular Transporters Complex, Deliver and Release SiRNA in Cells. *Proc. Natl. Acad. Sci. U. S. A.* **2012**, *109* (33), 13171−13176.
(31) Wender, P. A.; Huttner, M. A.; Staveness, D.; Vargas, J. R.; Xu, A. F. Guanidinium-Rich, Glycerol-Derived Oligocarbonates: A New Class of Cell-Penetrating Molecular Transporters That Complex, Deliver, and Release SiRNA. *Mol. Pharmaceutics* **2015**, *12* (3), 742−750.
(32) Pavlovic, I.; Thakor, D. T.; Vargas, J. R.; McKinlay, C. J.; Hauke, S.; Anstaett, P.; Camuña, R. C.; Bigler, L.; Gasser, G.; Schultz, C.; et al. Cellular Delivery and Photochemical Release of a Caged Inositol-Pyrophosphate Induces PH-Domain Translocation in Cellulo. *Nat. Commun.* **2016**, *7*, 10622.
(33) Kiesewetter, M. K.; Shin, E. J.; Hedrick, J. L.; Waymouth, R. M. Organocatalysis: Opportunities and Challenges for Polymer Synthesis. *Macromolecules* **2010**, *43* (5), 2093−2107.
(34) Cooley, C. B.; Trantow, B. M.; Nederberg, F.; Kiesewetter, M. K.; Hedrick, J. L.; Waymouth, R. M.; Wender, P. A. Oligocarbonate Molecular Transporters: Oligomerization-Based Syntheses and Cell-Penetrating Studies. *J. Am. Chem. Soc.* **2009**, *131* (45), 16401−16403.
(35) McKinlay, C. J.; Vargas, J. R.; Blake, T. R.; Hardy, J. W.; Kanada, M.; Contag, C. H.; Wender, P. A.; Waymouth, R. M. Charge-Altering Releasable Transporters (CARTs) for the Delivery and Release of MRNA in Living Animals. *Proc. Natl. Acad. Sci. U. S. A.* **2017**, *114* (4), E448−E456.
(36) McKinlay, C. J.; Benner, N. L.; Haabeth, O. A.; Waymouth, R. M.; Wender, P. A. Enhanced MRNA Delivery into Lymphocytes Enabled by Lipid-Varied Libraries of Charge-Altering Releasable Transporters. *Proc. Natl. Acad. Sci. U. S. A.* **2018**, *115*, 201805358.
(37) Benner, N. L.; Near, K. E.; Bachmann, M. H.; Contag, C. H.; Waymouth, R. M.; Wender, P. A. Functional DNA Delivery Enabled by Lipid-Modified Charge-Altering Releasable Transporters (CARTs). *Biomacromolecules* **2018**, *19* (7), 2812−2824.
(38) Hebbard, C. F. F.; Wang, Y.; Baker, C. J.; Morrissey, J. H. Synthesis and Evaluation of Chromogenic and Fluorogenic Substrates for High-Throughput Detection of Enzymes That Hydrolyze

DOI: 10.1021/acscentsci.8b00470
ACS Cent. Sci. 2018, 4, 1394−1402

Inorganic Polyphosphate. *Biomacromolecules* **2014**, *15* (8), 3190−3196.
(39) Choi, S. H.; Collins, J. N. R.; Smith, S. A.; Davis-Harrison, R. L.; Rienstra, C. M.; Morrissey, J. H. Phosphoramidate End Labeling of Inorganic Polyphosphates: Facile Manipulation of Polyphosphate for Investigating and Modulating Its Biological Activities. *Biochemistry* **2010**, *49* (45), 9935−9941.
(40) Lynn, D. M.; Langer, R. Degradable Poly(β-Amino Esters): Synthesis, Characterization, and Self-Assembly with Plasmid DNA. *J. Am. Chem. Soc.* **2000**, *122* (44), 10761−10768.
(41) McKinlay, C. J.; Waymouth, R. M.; Wender, P. A. Cell-Penetrating, Guanidinium-Rich Oligophosphoesters: Effective and Versatile Molecular Transporters for Drug and Probe Delivery. *J. Am. Chem. Soc.* **2016**, *138* (10), 3510−3517.
(42) Deshapriya, I. K.; Stromer, B. S.; Pattammattel, A.; Kim, C. S.; Iglesias-Bartolome, R.; Gonzalez-Fajardo, L.; Patel, V.; Gutkind, J. S.; Lu, X.; Kumar, C. V. Fluorescent, Bioactive Protein Nanoparticles (Prodots) for Rapid, Improved Cellular Uptake. *Bioconjugate Chem.* **2015**, *26* (3), 396−404.
(43) Prosperi, E.; Croce, A. C.; Bottiroli, G.; Supino, R. Flow Cytometric Analysis of Membrane Permeability Properties Influencing Intracellular Accumulation and Efflux of Fluorescein. *Cytometry* **1986**, *7* (1), 70−75.
(44) Prosperi, E. Intracellular Turnover of Fluorescein Diacetate. Influence of Membrane Ionic Gradients on Fluorescein Efflux. *Histochem. J.* **1990**, *22* (4), 227−233.
(45) Smith, S. A.; Morrissey, J. H. Sensitive Fluorescence Detection of Polyphosphate in Polyacrylamide Gels Using 4′,6-Diamidino-2-Phenylindol. *Electrophoresis* **2007**, *28* (19), 3461−3465.
(46) Aschar-Sobbi, R.; Abramov, A. Y.; Diao, C.; Kargacin, M. E.; Kargacin, G. J.; French, R. J.; Pavlov, E. High Sensitivity, Quantitative Measurements of Polyphosphate Using a New DAPI-Based Approach. *J. Fluoresc.* **2008**, *18* (5), 859−866.
(47) Dick, E.; Matsa, E.; Bispham, J.; Reza, M.; Guglieri, M.; Staniforth, A.; Watson, S.; Kumari, R.; Lochmüller, H.; Young, L.; et al. Two New Protocols to Enhance the Production and Isolation of Human Induced Pluripotent Stem Cell Lines. *Stem Cell Res.* **2011**, *6* (2), 158−167.
(48) Matsa, E.; Rajamohan, D.; Dick, E.; Young, L.; Mellor, I.; Staniforth, A.; Denning, C. Drug Evaluation in Cardiomyocytes Derived from Human Induced Pluripotent Stem Cells Carrying a Long QT Syndrome Type 2 Mutation. *Eur. Heart J.* **2011**, *32* (8), 952−962.
(49) Morimoto, D.; Tomita, T.; Kuroda, S.; Higuchi, C.; Kato, S.; Shiba, T.; Nakagami, H.; Morishita, R.; Yoshikawa, H. Inorganic Polyphosphate Differentiates Human Mesenchymal Stem Cells into Osteoblastic Cells. *J. Bone Miner. Metab.* **2010**, *28* (4), 418−423.
(50) Seidlmayer, L. K.; Gomez-Garcia, M. R.; Blatter, L. A.; Pavlov, E.; Dedkova, E. N. Inorganic Polyphosphate Is a Potent Activator of the Mitochondrial Permeability Transition Pore in Cardiac Myocytes. *J. Gen. Physiol.* **2012**, *139* (5), 321−331.
(51) Wender, P. A.; Huttner, M. A.; Staveness, D.; Vargas, J. R.; Xu, A. F. Guanidinium-Rich, Glycerol-Derived Oligocarbonates: A New Class of Cell-Penetrating Molecular Transporters That Complex, Deliver, and Release SiRNA. *Mol. Pharmaceutics* **2015**, *12* (3), 742−750.
(52) Müller, F.; Mutch, N. J.; Schenk, W. A.; Smith, S. A.; Esterl, L.; Spronk, H. M.; Schmidbauer, S.; Gahl, W. A.; Morrissey, J. H.; Renné, T. Platelet Polyphosphates Are Proinflammatory and Procoagulant Mediators In Vivo. *Cell* **2009**, *139* (6), 1143−1156.
(53) Ansevin, A. T.; Macdonald, K. K.; Smith, C. E.; Hnilica, L. S. Mechanics of Chromatin Template Activation. Physical Evidence for Destabilization of Nucleoproteins by Polyanions. *J. Biol. Chem.* **1975**, *250* (1), 281−289.
(54) Crouchet, E.; Saad, R.; Affolter-Zbaraszczuk, C.; Ogier, J.; Baumert, T. F.; Schuster, C.; Meyer, F. Composite Vector Formulation for Multiple SiRNA Delivery as a Host Targeting Antiviral in a Cell Culture Model of Hepatitis C Virus (HCV) Infection. *J. Mater. Chem. B* **2017**, *5* (4), 858−865.
(55) Contag, C. H.; Spilman, S. D.; Contag, P. R.; Oshiro, M.; Eames, B.; Dennery, P.; Stevenson, D. K.; Benaron, D. A. Visualizing Gene Expression in Living Mammals Using a Bioluminescent Reporter. *Photochem. Photobiol.* **1997**, *66* (4), 523−531.
(56) Lorenz, B.; Schröder, H. C. Mammalian Intestinal Alkaline Phosphatase Acts as Highly Active Exopolyphosphatase. *Biochim. Biophys. Acta, Protein Struct. Mol. Enzymol.* **2001**, *1547* (2), 254−261.
(57) Vollmayer, P.; Clair, T.; Goding, J. W.; Sano, K.; Servos, J.; Zimmermann, H. Hydrolysis of Diadenosine Polyphosphates by Nucleotide Pyrophosphatases/Phosphodiesterases. *Eur. J. Biochem.* **2003**, *270* (14), 2971−2978.
(58) Zhou, X.; Arthur, G. Improved Procedures for the Determination of Lipid Phosphorus by Malachite Green. *J. Lipid Res.* **1992**, *33* (8), 1233−1236.
(59) Blanco, E.; Shen, H.; Ferrari, M. Principles of Nanoparticle Design for Overcoming Biological Barriers to Drug Delivery. *Nat. Biotechnol.* **2015**, *33* (9), 941−951.
(60) Nel, A. E.; Mädler, L.; Velegol, D.; Xia, T.; Hoek, E. M. V.; Somasundaran, P.; Klaessig, F.; Castranova, V.; Thompson, M. Understanding Biophysicochemical Interactions at the Nano−Bio Interface. *Nat. Mater.* **2009**, *8* (7), 543−557.
(61) Sun, T.; Zhang, Y. S.; Pang, B.; Hyun, D. C.; Yang, M.; Xia, Y. Engineered Nanoparticles for Drug Delivery in Cancer Therapy. *Angew. Chem., Int. Ed.* **2014**, *53* (46), 12320−12364.

DOI: 10.1021/acscentsci.8b00470
ACS Cent. Sci. 2018, 4, 1394−1402